

Inflection-Point Inflation in a Hyper-Charge Oriented  $U(1)_X$   
Model

N. Okada – University of Alabama

S. Okada – Yamagata University

D. Raut – University of Alabama

Deposited 05/14/2019

Citation of published version:

Okada, N., Okada, S., Raut, D. (2017): Inflection-Point Inflation in a Hyper-Charge Oriented  $U(1)_X$  Model. *Physical Review D*, 95(5).

DOI: <https://doi.org/10.1103/PhysRevD.95.055030>

**Inflection-point inflation in a hyper-charge oriented  $U(1)_X$  model**Nobuchika Okada,<sup>1</sup> Satomi Okada,<sup>2</sup> and Digesh Raut<sup>1</sup><sup>1</sup>*Department of Physics and Astronomy, University of Alabama, Tuscaloosa AL35487, USA*<sup>2</sup>*Graduate School of Science and Engineering, Yamagata University, Yamagata 990-8560, Japan*

(Received 14 February 2017; published 31 March 2017)

Inflection-point inflation is an interesting possibility to realize a successful slow-roll inflation when inflation is driven by a single scalar field, with its value during inflation below the Planck mass ( $\phi_I \lesssim M_{\text{Pl}}$ ). In order for a renormalization group (RG) improved effective  $\lambda\phi^4$  potential to develop an inflection point, the running quartic coupling  $\lambda(\phi)$  must exhibit a minimum with an almost vanishing value in its RG evolution, namely  $\lambda(\phi_I) \simeq 0$  and  $\beta_\lambda(\phi_I) \simeq 0$ , where  $\beta_\lambda$  is the beta function of the quartic coupling. In this paper, we consider the inflection-point inflation in the context of the minimal  $U(1)_X$  extended Standard Model (SM), a generalization of the minimal  $U(1)_{B-L}$  model, where the  $U(1)_X$  symmetry is realized as a linear combination of the SM  $U(1)_Y$  and the  $U(1)_{B-L}$  gauge symmetries. We identify the  $U(1)_X$  Higgs field with the inflaton field. For successful inflection-point inflation to be consistent with the current cosmological observations, the mass ratios among the  $U(1)_X$  gauge boson, the right-handed neutrinos, and the  $U(1)_X$  Higgs boson are fixed. Focusing on the case that the  $U(1)_X$  gauge symmetry is mostly oriented towards the SM  $U(1)_Y$  direction, we investigate a consistency between the inflationary predictions and the latest LHC Run 2 results on the search for a narrow resonance with the dilepton final state. In addition, the inflection-point inflation provides a unique prediction for the running of the spectral index  $\alpha \simeq -2.7 \times 10^{-3} (\frac{60}{N})^2$  ( $N$  is the e-folding number), which can be tested in the near future.

DOI: [10.1103/PhysRevD.95.055030](https://doi.org/10.1103/PhysRevD.95.055030)**I. INTRODUCTION**

The inflationary universe is the standard paradigm in modern cosmology [1–4], which provides not only solutions to various problems in the Standard Big Bang Cosmology, such as the flatness and horizon problems, but also the primordial density fluctuations which seed the formation of the large scale structure of the universe we see today. In a simple inflationary scenario known as slow-roll inflation, inflation is driven by a single scalar field (an inflaton) when it slowly rolls down to its potential minimum. During the slow roll, the energy density of the universe is dominated by the inflaton potential energy, which drives accelerated expansion of the universe, namely, cosmological inflation. After the end of inflation, the inflaton decays to Standard Model (SM) particles to reheat the universe to initiate the Standard Big Bang cosmology.

The slow-roll inflation requires the inflaton potential to be sufficiently flat in the inflationary epoch. In a simple inflationary scenario such as chaotic inflation, a flat potential is realized by taking an initial inflaton value to be of the trans-Planckian scale. However, from the field theoretical point of view, it may be more appealing to consider the small-field inflation (SFI) scenario, where the initial inflaton value is smaller than the Planck mass and possible higher-dimensional Planck suppressed operators are less important to the inflationary predictions. Hybrid inflation [5] is a well known example of the SFI [5], where a flat direction of the scalar potential is realized with multiple scalar fields. When one considers the SFI driven by a single scalar field, the

so-called inflection-point inflation [6–8] is an interesting possibility. If the inflaton potential exhibits an inflection point, the slow-roll inflation epoch can be realized with the initial inflaton value in the immediate vicinity of the inflection point.

From a particle physics point of view, an inflation scenario seems more compelling if the inflaton field plays another important role in particle physics models, such as the Higgs inflation scenario [9–11] in which the SM Higgs field is identified with the inflaton field. When the SM is extended with some extra gauge groups, or unified gauged groups, such models always include an extra Higgs field, in addition to the SM Higgs field, to spontaneously break the gauge symmetries down to the SM one. Similarly to the Higgs inflation scenario, it is interesting if we can identify the extra Higgs field with the inflaton. The extra Higgs field usually has Yukawa couplings with some fermions, in addition to the gauge and quartic couplings, just like the SM Higgs doublet. As will be discussed below, this gauge-Higgs-Yukawa system is essential to realize the inflection-point inflation with the identification of the Higgs field as the inflaton.

Let us consider a renormalization-group (RG) improved effective Higgs/inflaton potential [12]. During the inflation, we assume that the inflaton value is much larger than its vacuum expectation value (VEV) at the potential minimum, so that the inflaton potential is dominated by its quartic term of the form,

$$V(\phi) = \frac{1}{4}\lambda(\phi)\phi^4, \quad (1.1)$$

where  $\phi$  denotes the inflaton field, and  $\lambda(\phi)$  is the running quartic coupling. If the RG running of the inflaton quartic coupling first decreases towards high energy and then increases, the inflection point is realized in the vicinity of the minimum point of the running quartic coupling, where both the quartic coupling and its beta function become vanishingly small [7,8].<sup>1</sup> In the vicinity of the inflection point, the running quartic coupling obeys the (one-loop) RG equation of the form,

$$16\pi^2 \frac{d\lambda}{d\ln\phi} \simeq C_g g^4 - C_Y Y^4, \quad (1.2)$$

where  $g$  and  $Y$  are the gauge and Yukawa couplings, respectively, and  $C_g$  and  $C_Y$  are positive coefficients whose actual values are calculable once the particle content of the model is defined. Here, we have neglected terms proportional to  $\lambda$  ( $\lambda^2$  term and the anomalous dimension term) because the SFI requires the quartic coupling  $\lambda \propto g^6$ , as will be shown later. Hence, the quantum corrections to the effective Higgs potential are dominated by the gauge and Yukawa interactions. Realization of the inflection point requires a vanishingly small beta function at the initial inflaton value, namely  $C_g g - C_Y Y = 0$ . This condition leads to a relationship between  $g$  and  $Y$ , or in other words, the mass ratio of the gauge boson to the fermion in the Higgs model is fixed. Since the Higgs quartic coupling at low energy is evaluated by solving the RG equation, the resultant Higgs mass also has a unique relationship to the gauge and the fermion masses. Therefore, in the inflection-point inflation scenario with the Higgs field as the inflaton, there is a correlation between the very high energy physics of inflation and the low energy particle phenomenology.

Recently, two of the authors of this paper (N. O. and D. R.) have investigated the inflection-point inflation in the minimal gauged  $B-L$  (baryon number minus lepton number) extension of the SM [15], with the  $B-L$  Higgs field as the inflaton field [16]. In order to realize the successful inflection-point inflation, we have obtained the predictions for the mass spectrum for the  $B-L$  gauge boson ( $Z'$  boson), the right-handed neutrinos, and the  $B-L$  Higgs boson as a function of the initial inflaton value ( $\phi_I$ ) and the inflaton/Higgs VEV ( $v_{BL}$ ). Considering the reheating after inflation with the fixed particle mass spectrum, we have identified the allowed parameter regions to satisfy the big bang nucleosynthesis constraint. We have found that the entire parameter region for  $m_{Z'} \lesssim 500$  GeV can be tested by the future collider experiments such as the High-Luminosity Large Hadron Collider (LHC) [17] and the search for hidden particles (SHiP) [18] experiments.

In this paper, we generalize the minimal  $B-L$  model to the so-called nonexotic  $U(1)_X$  extension of the SM [19].

<sup>1</sup>In the context of the  $\lambda\phi^4$  inflation with non-minimal gravitational coupling [13], similar conditions have been derived to ensure the stability of the inflaton potential [14].

The nonexotic  $U(1)_X$  model is the most general extension of the SM with an extra anomaly-free  $U(1)$  gauge symmetry, which is described as a linear combination of the SM  $U(1)_Y$  and the  $U(1)_{B-L}$  gauge groups. The particle content of the model is the same as the one in the minimal  $B-L$  model, except for the generalization of the  $U(1)_X$  charge assignment for particles. The orientation of the  $U(1)_X$  gauge group is characterized by a  $U(1)_X$  charge of the SM Higgs doublet ( $x_H$ ). For example,  $x_H = 0$  is the  $U(1)_{B-L}$  limit, while the  $U(1)_{B-L}$  gauge group is oriented to the SM  $U(1)_Y$  direction for  $|x_H| \gg 1$ . In this context, we investigate the inflection-point inflation with the identification of the  $U(1)_X$  Higgs field as the inflaton. As we will discuss in the following, the inflation analysis weakly depends on  $x_H$ , and hence, our results are similar to those in Ref. [16]. However, there is a sharp contrast in low energy phenomenologies, in particular, the  $U(1)_X$  gauge boson phenomenology at the LHC. An upper bound on the  $U(1)_{B-L}$  gauge coupling,  $g_{BL} \lesssim 0.01$ , has been obtained from theoretical consistencies in Ref. [16]. The  $Z'$  boson, with such a small coupling, can be explored in future collider experiments only for a small mass region such as  $m_{Z'} \lesssim 500$  GeV. For this case in the inflection-point inflation scenario, the reheating temperature is estimated to be  $T_R \lesssim 1$  GeV [16]. Such a low reheating temperature may not be desirable in terms of thermal dark matter physics and the baryogenesis scenario. On the other hand, in the  $U(1)_X$  generalization, the coupling of the  $Z'$  boson with the SM fermions is controlled by  $g_X x_H$  for  $|x_H| \gtrsim 1$ , with  $g_X$  being the  $U(1)_X$  gauge coupling, and therefore the  $Z'$  boson coupling becomes sizable for  $|x_H| \gg 1$ . In this paper, we will investigate the inflection-point inflation for this hypercharge oriented  $U(1)_X$  extension of the SM, which opens up a possibility to explore the mass region of  $m_{Z'} > 1$  TeV at the LHC Run 2, while successfully realizing the inflection-point inflation.

The paper is organized as follows. In the next section, we give a brief review of the slow-roll inflation. In Sec. III, we present the inflationary predictions for the scenario, where the inflaton potential exhibits an inflection-pointlike behavior during the slow roll. In Sec. IV, we consider the minimally gauged  $B-L$  extension of the SM, where the  $B-L$  Higgs field is identified with the inflaton field. To realize the inflection point in a Higgs/inflaton potential, we consider the RG improved effective Higgs/inflaton potential. In Sec. V, we consider the constraints on the model parameters from the big bang nucleosynthesis and the current collider experiments. We also discuss the prospects of testing the scenario in the future collider experiments, such as the High-Luminosity LHC and SHiP experiments. Section VI is devoted to conclusions.

## II. BASICS OF INFLECTION-POINT INFLATION

The inflationary slow-roll parameters for the inflaton field ( $\phi$ ) are given by

$$\begin{aligned}\epsilon(\phi) &= \frac{M_P^2}{2} \left( \frac{V'}{V} \right)^2, & \eta(\phi) &= M_P^2 \left( \frac{V''}{V} \right), \\ \zeta^2(\phi) &= M_P^4 \frac{V'V'''}{V^2},\end{aligned}\quad (2.1)$$

where  $M_P = M_{\text{pl}}/\sqrt{8\pi} = 2.43 \times 10^{18}$  GeV is the reduced Planck mass,  $V$  is the inflaton potential, and the prime denotes the derivative with respect to  $\phi$ . The amplitude of the curvature perturbation  $\Delta_{\mathcal{R}}^2$  is given by

$$\Delta_{\mathcal{R}}^2 = \frac{1}{24\pi^2} \frac{1}{M_P^4} \left. \frac{V}{\epsilon} \right|_{k_0}, \quad (2.2)$$

which should satisfy  $\Delta_{\mathcal{R}}^2 = 2.195 \times 10^{-9}$  from the Planck 2015 results [20], with the pivot scale chosen at  $k_0 = 0.002 \text{ Mpc}^{-1}$ . The number of e-folds is defined as

$$N = \frac{1}{M_P^2} \int_{\phi_E}^{\phi_I} d\phi \frac{V}{V'}, \quad (2.3)$$

where  $\phi_I$  is the inflaton value at a horizon exit corresponding to the scale  $k_0$ , and  $\phi_E$  is the inflaton value at the end of inflation, which is defined by  $\epsilon(\phi_E) = 1$ . The value of  $N$  depends logarithmically on the energy scale during inflation, as well as on the reheating temperature, and it is typically taken to be 50–60.

The slow-roll approximation is valid as long as the conditions  $\epsilon \ll 1$ ,  $|\eta| \ll 1$ , and  $\zeta^2 \ll 1$  hold. In this case, the inflationary predictions are given by

$$n_s = 1 - 6\epsilon + 2\eta, \quad r = 16\epsilon, \quad \alpha = 16\epsilon\eta - 24\epsilon^2 - 2\zeta^2, \quad (2.4)$$

where  $n_s$ ,  $r$  and  $\alpha \equiv \frac{dn_s}{d \ln k}$  are the scalar spectral index, the tensor-to-scalar ratio and the running of the spectral index, respectively, which are evaluated at  $\phi = \phi_I$ . The Planck 2015 results [20] set an upper bound on the tensor-to-scalar ratio as  $r \lesssim 0.11$ , while the best fit value for the spectral index ( $n_s$ ) and the running of spectral index ( $\alpha$ ) are  $0.9655 \pm 0.0062$  and  $-0.0057 \pm 0.0071$ , respectively, at a 68% C.L.

In the SFI scenario, to realize the slow-roll inflation, the inflaton potential must exhibit an inflection-pointlike behavior, where the potential is very flat.<sup>2</sup> Setting the inflaton value at the horizon in the very flat region  $\phi_I = M$  of the potential, we approximate the inflaton potential by the following expansion around  $\phi = M^3$ :

<sup>2</sup>For a successful inflation scenario, it is not necessary for the potential to realize an *exact* inflection point. We only require the inflaton potential to exhibit a behavior of almost an inflection point.

<sup>3</sup>Although our parametrization of the inflaton potential is slightly different, most of the analysis in this section overlaps with that in Ref. [8].

$$V(\phi) \simeq V_0 + V_1(\phi - M) + \frac{V_2}{2}(\phi - M)^2 + \frac{V_3}{6}(\phi - M)^3, \quad (2.5)$$

where  $V_0$  is a constant and  $V_1$ ,  $V_2$ , and  $V_3$  are the first, second, and third derivatives of the inflaton potential evaluated at  $\phi = M$ . When  $V_1$  and  $V_2$  are vanishingly small, the inflaton potential exhibits the inflection-pointlike behavior. From Eqs. (2.1) and (2.5), the slow-roll parameters are then given by

$$\begin{aligned}\epsilon(M) &\simeq \frac{M_P^2}{2} \left( \frac{V_1}{V_0} \right)^2, & \eta(M) &\simeq M_P^2 \left( \frac{V_2}{V_0} \right), \\ \zeta^2(M) &= M_P^4 \frac{V_1 V_3}{V_0^2},\end{aligned}\quad (2.6)$$

where we have used the approximation  $V(M) \simeq V_0$ . Similarly, the power spectrum  $\Delta_{\mathcal{R}}^2$  is expressed as

$$\Delta_{\mathcal{R}}^2 \simeq \frac{1}{12\pi^2} \frac{V_0^3}{M_P^6 V_1^2}. \quad (2.7)$$

Using the constraint  $\Delta_{\mathcal{R}}^2 = 2.195 \times 10^{-9}$  from the Planck 2015 results, we can express  $V_1$  and  $V_2$  as

$$\begin{aligned}\frac{V_1}{M^3} &\simeq 1961 \left( \frac{M}{M_P} \right)^3 \left( \frac{V_0}{M^4} \right)^{3/2}, \\ \frac{V_2}{M^2} &\simeq -1.725 \times 10^{-2} \left( \frac{1 - n_s}{1 - 0.9655} \right) \left( \frac{M}{M_P} \right)^2 \left( \frac{V_0}{M^4} \right),\end{aligned}\quad (2.8)$$

where we have used  $V(M) \simeq V_0$  and  $\epsilon(M) \ll |\eta(M)|$ , as will be verified later. For the following analysis we set  $n_s = 0.9655$  at the center value from the Planck 2015 results [20].

We define the inflaton value ( $\phi_E$ ) at the end of inflation by  $\epsilon(\phi_E) = 1$ . Using Eq. (2.3), the e-folding number ( $N$ ) is given by

$$\begin{aligned}N &= \frac{2V_0}{M_P^2 \sqrt{-V_2^2 + 2V_1 V_3}} \\ &\times \arctan \left( \frac{V_2 + V_3(\phi - M)}{\sqrt{-V_2^2 + 2V_1 V_3}} \right) \Bigg|_{\phi=M(1-\delta_E)}^{\phi=M},\end{aligned}\quad (2.9)$$

where we have parametrized  $\phi_E$  as  $\phi_E/M = 1 - \delta_E$  with  $0 < \delta_E < 1$ . The inflection-pointlike behavior of the inflaton potential requires  $V_1, V_2 \simeq 0$ , and  $V_3 > 0$ , so that we can approximate  $-V_2^2 + 2V_1 V_3 \simeq 2V_1 V_3$ . This approximation is justified later. As we will also show later,  $V_2, \sqrt{2V_1 V_3} \ll V_3 M \delta_E$ , and hence the e-folding number, is approximated as

$$N \simeq \frac{2V_0}{M_P^2 \sqrt{2V_1 V_3}} \arctan \left[ \frac{V_3 M \delta_E}{\sqrt{2V_1 V_3}} \right] \simeq \pi \frac{V_0}{M_P^2 \sqrt{2V_1 V_3}}. \quad (2.10)$$

TABLE I. The particle content of the minimal  $U(1)_X$  extended SM. In addition to the SM particle content ( $i = 1, 2, 3$ ), the three right-handed neutrinos ( $N_R^i$  ( $i = 1, 2, 3$ )) and the  $U(1)_X$  Higgs field ( $\Phi$ ), which is identified with the inflaton, are introduced. The extra  $U(1)_X$  gauge group is defined with a linear combination of the SM  $U(1)_Y$  and the  $U(1)_{B-L}$  gauge groups, and the  $U(1)_X$  charges of fields are determined by two real parameters,  $x_H$  and  $x_\Phi$ . Without the loss of generality, we fix  $x_\Phi = 1$  throughout this paper.

	$SU(3)_c$	$SU(2)_L$	$U(1)_Y$	$U(1)_X$
$q_L^i$	<b>3</b>	<b>2</b>	1/6	$(1/6)x_H + (1/3)x_\Phi$
$u_R^i$	<b>3</b>	<b>1</b>	2/3	$(2/3)x_H + (1/3)x_\Phi$
$d_R^i$	<b>3</b>	<b>1</b>	-1/3	$(-1/3)x_H + (1/3)x_\Phi$
$\ell_L^i$	<b>1</b>	<b>2</b>	-1/2	$(-1/2)x_H - x_\Phi$
$e_R^i$	<b>1</b>	<b>1</b>	-1	$(-1)x_H - x_\Phi$
$H$	<b>1</b>	<b>2</b>	-1/2	$(-1/2)x_H$
$N_R^i$	<b>1</b>	<b>1</b>	0	$-x_\Phi$
$\Phi$	<b>1</b>	<b>1</b>	0	$+2x_\Phi$

Using Eq. (2.8),  $V_3$  is then given by

$$\frac{V_3}{M} \simeq 6.989 \times 10^{-7} \left(\frac{60}{N}\right)^2 \sqrt{\frac{V_0}{M^2 M_P^2}}. \quad (2.11)$$

From Eqs. (2.8) and (2.11), we find  $2V_1 V_3 \simeq 9.2(60/N)V_2^2$ , and  $-V_2^2 + 2V_1 V_3 \simeq 2V_1 V_3$  is a good approximation for  $N = 50\text{--}60$ .

Using Eqs. (2.4), (2.6), (2.8), and (2.11), we now express all inflationary predictions in terms  $V_0$ ,  $M$ , and  $N$ . From Eqs. (2.6) and (2.8), the tensor-to-scalar ratio ( $r$ ) is given by

$$r = 3.077 \times 10^7 \left(\frac{V_0}{M_P^4}\right). \quad (2.12)$$

The running of the spectral index ( $\alpha$ ) is found to be

$$\alpha \simeq -2\zeta^2(M) = -2.742 \times 10^{-3} \left(\frac{60}{N}\right)^2. \quad (2.13)$$

Note that this  $\alpha$  value is a unique prediction of the inflection-point inflation, independent of  $V_0$  and  $M$ . This prediction is consistent with the current experimental bound,  $\alpha = -0.0057 \pm 0.0071$  [20]. It is expected that future experiments can reduce the error to  $\pm 0.002$  [21], and therefore the prediction of the inflection-point inflation scenario can be tested in the future.

### III. THE INFLECTION-POINT $U(1)_X$ HIGGS INFLATION

The model we will investigate is the anomaly-free  $U(1)_X$  extension of the SM, which is based on the gauge group  $SU(3)_c \times SU(2)_L \times U(1)_Y \times U(1)_X$ . The particle content of the model is listed in Table I. The covariant derivative relevant to  $U(1)_Y \times U(1)_X$  is given by

$$D_\mu \equiv \partial_\mu - i(g_1 Y + \tilde{g} Q_X) B_\mu - i g_X Q_X Z'_\mu, \quad (3.1)$$

where  $Y$  ( $Q_X$ ) are the  $U(1)_Y$  ( $U(1)_X$ ) charge of a particle, and the gauge coupling  $\tilde{g}$  is introduced in association with a kinetic mixing between the two  $U(1)$  gauge bosons. Although we set  $\tilde{g}$  zero at the  $U(1)_X$  symmetry breaking scale, it is generated through the RG evolutions. The particle content includes three generations of right-hand neutrinos  $N_R^i$  and a  $U(1)_X$  Higgs field  $\Phi$ , in addition to the SM particle content. The  $U(1)_X$  gauge group is identified with a linear combination of the SM  $U(1)_Y$  and the  $U(1)_{B-L}$  gauge groups, and hence, the  $U(1)_X$  charges of fields are determined by two real parameters,  $x_H$  and  $x_\Phi$ . Note that in the model, the charge  $x_\Phi$  always appears as a product with the  $U(1)_X$  gauge coupling, and it is not an independent free parameter. Hence, we fix  $x_\Phi = 1$  throughout this paper. In this way, we reproduce the minimal  $B-L$  model with the conventional charge assignment as the limit of  $x_H \rightarrow 0$ .<sup>4</sup> The limit of  $x_H \rightarrow +\infty$  ( $-\infty$ ) indicates that the  $U(1)_X$  is (anti-) aligned to the SM  $U(1)_Y$  direction. The anomaly structure of the model is the same as the minimal  $B-L$  model and the model is free from all of the gauge and the gravitational anomalies in the presence of the three right-handed neutrinos.

The Yukawa sector of the SM is extended to have

$$\begin{aligned} \mathcal{L}_{\text{Yukawa}} \supset & - \sum_{i=1}^3 \sum_{j=1}^3 Y_D^{ij} \bar{\ell}_L^i H N_R^j \\ & - \frac{1}{2} \sum_{k=1}^3 Y_M^k \Phi \overline{N_R^{kC}} N_R^k + \text{H.c.}, \end{aligned} \quad (3.2)$$

where the first and second terms are the neutrino Dirac Yukawa coupling and the Majorana Yukawa coupling, respectively. Without loss of generality, the Majorana Yukawa couplings are already diagonalized in our basis. Once the  $U(1)_X$  Higgs field  $\Phi$  develops a nonzero VEV, the  $U(1)_X$  gauge symmetry is broken and the Majorana masses for the right-handed neutrinos are generated. Then, the seesaw mechanism [22] is automatically implemented in the model after the electroweak symmetry breaking.

The renormalizable scalar potential for the SM Higgs doublet ( $H$ ) and the  $U(1)_X$  Higgs ( $\Phi$ ) fields is given by

$$\begin{aligned} V = & \lambda_H \left( H^\dagger H - \frac{v_h^2}{2} \right)^2 + \lambda_\Phi \left( \Phi^\dagger \Phi - \frac{v_X^2}{2} \right)^2 \\ & + \lambda_{\text{mix}} \left( H^\dagger H - \frac{v_h^2}{2} \right) \left( \Phi^\dagger \Phi - \frac{v_X^2}{2} \right), \end{aligned} \quad (3.3)$$

<sup>4</sup>For  $x_H = -4/5$  and  $x_H = -2$ , the  $U(1)_X$  gauge group can arise from breaking of the  $SO(10)$  grand unified gauge group into the Standard Model one via the  $SU(5) \times U(1)_X$  for the standard  $SU(5)$  and the flipped  $SU(5)$  subgroups of the  $SO(10)$ , respectively.

where all quartic couplings are chosen to be positive. At the potential minimum, the Higgs fields develop their VEVs as

$$\langle H \rangle = \begin{pmatrix} \frac{v_h}{\sqrt{2}} \\ 0 \end{pmatrix}, \quad \langle \Phi \rangle = \frac{v_X}{\sqrt{2}}. \quad (3.4)$$

Associated with the  $U(1)_X$  symmetry breaking (as well as the electroweak symmetry breaking), the  $U(1)_X$  gauge boson ( $Z'$  boson), the right-handed Majorana neutrinos, and the  $U(1)_X$  Higgs boson ( $\phi$ ) acquire their masses as

$$m_{Z'} = g_X \sqrt{4v_X^2 + \frac{x_H^2}{4} v_h^2} \simeq 2g_X v_X, \\ m_{N^i} = \frac{1}{\sqrt{2}} Y_M^i v_X, \quad m_\phi = \sqrt{2\lambda_\Phi} v_X, \quad (3.5)$$

where  $v_h = 246$  GeV is the SM Higgs VEV, and we have used the LEP constraint [23]  $v_X^2 \gg v_h^2$ . Because of the LEP constraint, the mass mixing of the  $Z'$  boson with the SM  $Z$  boson is very small, and we neglect it in our analysis in this paper.

We identify the physical  $U(1)_X$  Higgs field ( $\phi$ ) with the inflaton, which is defined as  $\Phi = (\phi + v_X)/\sqrt{2}$  in the unitary gauge, and consider the inflation trajectory  $\phi \gg v_X$ ,  $v_h$  and  $H = 0$  in the scalar potential in Eq. (3.3). In our analysis, we employ the RG improved effective potential along this inflation trajectory, which is dominated by the inflaton quartic term and given by

$$V(\phi) = \frac{1}{4} \lambda(\phi) \phi^4, \quad (3.6)$$

where  $\lambda(\phi)$  is the solution to the RG equation listed in the Appendix. With the RG improved effective potential, we express the coefficients in the expansion of Eq. (2.5) as

$$\frac{V_1}{M^3} = \frac{1}{4} (4\lambda_\Phi + \beta_{\lambda_\Phi}), \\ \frac{V_2}{M^2} = \frac{1}{4} (12\lambda_\Phi + 7\beta_{\lambda_\Phi} + M\beta'_{\lambda_\Phi}), \\ \frac{V_3}{M} = \frac{1}{4} (24\lambda_\Phi + 26\beta_{\lambda_\Phi} + 10M\beta'_{\lambda_\Phi} + M^2\beta''_{\lambda_\Phi}), \quad (3.7)$$

where the prime denotes  $d/d\phi$ , and  $\beta_{\lambda_\Phi}$  is the beta function of the quartic coupling  $\lambda_\Phi$ , given by

$$\beta_{\lambda_\Phi} = \frac{1}{(4\pi)^2} \left[ \lambda_\Phi \left\{ 20\lambda_\Phi + 2 \sum_{i=1}^3 (Y_M^i)^2 - 48(\tilde{g}^2 + g_X^2) \right\} \right. \\ \left. + 2\lambda_{\text{mix}}^2 + 96(\tilde{g}^2 + g_X^2)^2 - \sum_{i=1}^3 (Y_M^i)^4 \right]. \quad (3.8)$$

Using  $V_1/M^3 \simeq 0$  and  $V_2/M^2 \simeq 0$  to realize the inflection-pointlike behavior of the inflaton effective potential, we obtain

$$\beta_{\lambda_\Phi}(M) \simeq -4\lambda_\Phi(M), \quad M\beta'_{\lambda_\Phi}(M) \simeq 16\lambda_\Phi(M). \quad (3.9)$$

For the couplings being in the perturbative regime, we evaluate  $M^2\beta''_{\lambda_\Phi}(M) \simeq -M\beta'_{\lambda_\Phi}(M) \simeq -16\lambda_\Phi(M)$  as a good approximation. Hence the last equation in Eq. (3.7) is simplified to be  $V_3/M \simeq 16\lambda_\Phi(M)$ , and Eq. (2.11) leads to

$$\lambda_\Phi(M) \simeq 4.770 \times 10^{-16} \left( \frac{M}{M_P} \right)^2 \left( \frac{60}{N} \right)^4, \quad (3.10)$$

where we have used  $V_0 \simeq (1/4)\lambda_\Phi(M)M^4$ , for  $M \lesssim M_P$ ,  $\lambda_\Phi(M)$  is found to be very small.

In evaluating  $\beta_{\lambda_\Phi}(M)$ , we simply assume  $\lambda_{\text{mix}}(M)$  is negligibly small. Although we have set  $\tilde{g}(v_X) = 0$ , non-vanishing  $\tilde{g}(M)$  is generated through its RG evolution through its beta function consisting of two terms: one is proportional to  $\tilde{g}$  and the other is proportional to  $g_X$ . However, as we will see later, the inflection-point inflation requires  $g_X(M) \ll 1$ , and hence,  $\tilde{g}$  stays negligibly small at any scale. As a result, Eq. (3.9) with Eq. (3.10) leads to  $\beta_{\lambda_\Phi}(M) \simeq 0$ , and we find

$$Y_M(M) \simeq 32^{1/4} g_X(M), \quad (3.11)$$

where we have taken the degenerate Yukawa couplings for three right-handed neutrinos  $Y_M \equiv Y_M^1 = Y_M^2 = Y_M^3$ , for simplicity. Therefore, the mass ratio between the right-handed neutrinos and the  $Z'$  gauge boson is fixed to realize a successful inflection-point inflation.

Now RG equations for  $\lambda_\Phi$ ,  $g_X$ , and  $Y_M$  at the 1-loop level are approximately given by

$$16\pi^2 \frac{d\lambda_\Phi}{d \ln \phi} \simeq 96g_X^4 - 3Y_M^4, \\ 16\pi^2 \frac{dg_X}{d \ln \phi} = \left( \frac{72 + 64x_H + 41x_H^2}{6} \right) g_X^3, \\ 16\pi^2 \frac{dY_M}{d \ln \phi} \simeq Y_M \left( \frac{5}{2} Y_M^2 - 6g_X^2 \right). \quad (3.12)$$

Using the second equation in Eq. (3.9) and Eqs. (3.10)–(3.12), we express the  $U(1)_X$  gauge coupling at  $\phi = M$  as

$$g_X(M) \simeq \frac{1.511 \times 10^{-2}}{(93 + 256x_H + 164x_H^2)^{1/6}} \left( \frac{M}{M_P} \right)^{1/3} \left( \frac{60}{N} \right)^{2/3}. \quad (3.13)$$

Finally, from Eqs. (2.12) and (3.10), the tensor-to-scalar ratio ( $r$ ) is given by

$$r \simeq 3.670 \times 10^{-9} \left( \frac{M}{M_P} \right)^6, \quad (3.14)$$

which is very small, as expected for the SFI scenario.

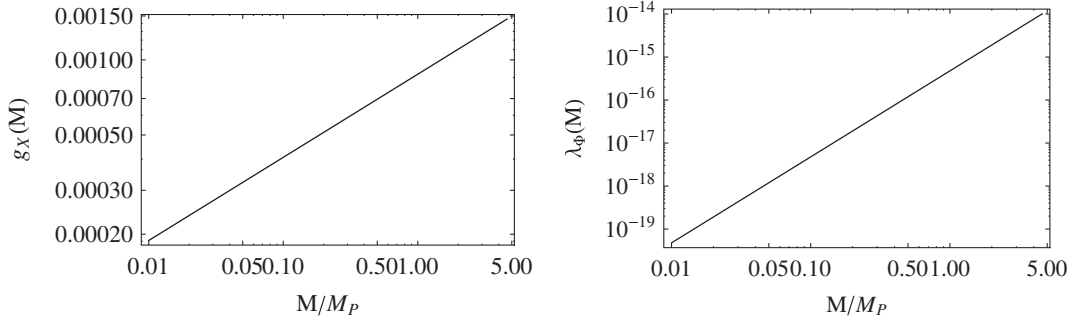


FIG. 1. The left and right panels show the  $U(1)_X$  gauge coupling [ $g_X(M)$ ] and the inflaton quartic coupling [ $\lambda_\Phi(M)$ ] as a function of  $M/M_P$ , respectively, for a fixed  $x_H = 400$ .

At the end of inflation,  $\epsilon(\phi_E)$  is explicitly given by

$$\begin{aligned} \epsilon(\phi_E) &= \frac{M_P^2}{2V_0^2} \left( V_1 - V_2 M \delta_E + \frac{V_3}{2} M^2 \delta_E^2 \right)^2 \\ &\simeq \frac{M_P^2 M^6 \delta_E^2}{2V_0^2} \left( -\frac{V_2}{M^2} + \frac{V_3}{2M} \delta_E \right)^2. \end{aligned} \quad (3.15)$$

We evaluate  $\delta_E$  from  $\epsilon(\phi_E) = 1$ . If we assume that the first term dominates in the parenthesis of the final expression above, we find  $\delta_E \gg 1$  by using Eqs. (2.8), (2.11), and (3.10), which is inconsistent with  $0 < \delta_E < 1$ . Therefore, the second term must dominate, and hence, we obtain

$$\delta_E \simeq 0.210 \left( \frac{M}{M_P} \right)^{1/2}, \quad (3.16)$$

by using Eqs. (2.11) and (3.10).

Before presenting our numerical results, let us check the consistency of our analysis. In the previous section we have approximated the inflaton potential by Eq. (2.5), neglecting the higher order terms. For consistency, we need to check if the contribution of higher order terms can actually be neglected in our model. Consider the following expansion of inflaton potential at  $\phi = M$ ,

$$V(\phi) = \sum_{n=0} \frac{V^{(n)}}{n!} (\phi - M)^n, \quad (3.17)$$

where  $V^{(n)}$  is the  $n$ th derivative of the potential evaluated at  $\phi = M$ . As has been discussed in the previous section,  $V_1 = V^{(1)}$  and  $V_2 = V^{(2)}$  are fixed by the experimental values of the scalar power spectrum ( $\Delta_{\mathcal{R}}^2$ ) and the spectral index ( $n_s$ ), respectively. For the consistency of our previous analysis, we require that the terms  $V^{(4)}$  and higher contribute negligibly in the determination of  $\delta_E$  compared to  $V_3$  at the end of inflation. Using Eqs. (2.1) and (3.17),  $\epsilon(\phi_E)$  is expressed as

$$\begin{aligned} \epsilon(\phi_E) &\simeq \frac{M_P^2}{2V_0^2} \left( \sum_{n=1} \frac{V^{(n)}}{(n-1)!} (\phi - M)^{n-1} \right)^2 \\ &\simeq \frac{M_P^2}{2V_0^2} \left( \frac{V_3}{2} M^2 \delta_E^2 + \sum_{n=4} \frac{V^{(n)}}{(n-1)!} (M \delta_E)^{n-1} \right)^2, \end{aligned} \quad (3.18)$$

where we have used  $V(\phi_E) \simeq V_0$ . This leads to the constraint

$$\delta_E^{(p-3)} < \left| \frac{(p-1)! V^{(3)}}{2 V^{(p)}} M^{3-p} \right|. \quad (3.19)$$

where  $p \geq 4$ . To proceed further we need to evaluate Eq. (3.19) explicitly for the minimal  $U(1)_X$  model. As has been shown previously in this section, all of the higher order derivatives of the potential can be approximately given by  $V^{(n)} M^{n-4} \simeq C_n \lambda(M)$ , where  $C_n$  is a constant. For example,  $C_4 = 96$  and  $C_5 = 184$ . We find that the most severe bound for both cases is from the  $V^{(4)}$  term. Using the Eqs. in (3.16), we obtain an upper bound on  $M < 5.67 M_P$ .

Let us now present the numerical results of the inflection-point  $U(1)_X$  Higgs inflation scenario. For the rest of the paper, we employ the e-folding number  $N = 60$ . We set  $\tilde{g}(v_X) = 0$  and choose  $\lambda_{\text{mix}}(M)$  to be  $\lambda_{\text{mix}}^2 \ll 48 g_X^4$ , and hence, all of our results presented in the rest of this section are controlled by only three parameters,  $M$ ,  $x_H$ , and  $v_X$ .

In Fig. 1, we show the  $U(1)_X$  gauge coupling (left) and the inflaton quartic coupling (right) at  $\phi = M$  as a function of  $M$  [see Eqs. (3.10) and (3.11)]. Here, we have fixed  $x_H = 400$ , which is motivated by the LHC phenomenology to be discussed in the next section.

In Fig. 2, we plot the running quartic coupling  $\lambda_\Phi(\phi)$  (left) and the RG improved effective inflaton/Higgs potential (right). Here we have fixed  $M = M_P$  and  $x_H = 400$ , which corresponds to  $g_X(M) = 8.760 \times 10^{-4}$ ,  $Y_M(M) = 2.103 \times 10^{-3}$ , and  $\lambda_\Phi(M) \simeq 4.770 \times 10^{-16}$ . In the left panel, the dashed line indicates  $\lambda_\Phi = 0$ . In the right panel, we see the inflection-pointlike behavior of the inflaton potential around  $\phi = M$ , marked with a dashed-dotted vertical line.

Here let us look at the inflationary predictions of our scenario. The prediction for the tensor-to-scalar ratio ( $r$ ) is given by Eq. (3.14). For the upper bound on  $M < 5.67 M_P$ , the resultant tensor-to-scalar ratio is given by  $r < 3.047 \times 10^{-5}$ , which is too small to test in future experiments. However, as discussed in the previous section, the inflection-point inflation predicts the running of the spectral index to be  $\alpha \simeq -2.742 \times 10^{-3}$ , independently of  $M$ . This predicted value is within the reach of future precision measurements [21].

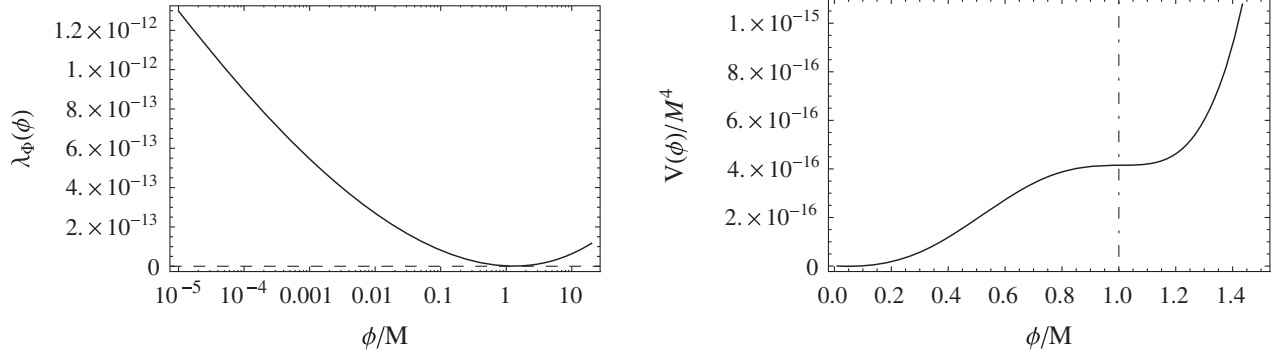


FIG. 2. Left panel shows the RG running of the  $U(1)_X$  Higgs/inflaton quartic coupling plotted against the normalized energy scale  $\phi/M$ . Here we have fixed  $M = M_P$  and  $x_H = 400$ , which corresponds to  $g_X(M) = 8.756 \times 10^{-4}$ ,  $Y_M(M) = 2.478 \times 10^{-3}$ , and  $\lambda_\Phi(M) \approx 4.770 \times 10^{-16}$ . The dashed horizontal line indicates  $\lambda = 0$ . The right panel shows the corresponding RG improved inflaton potential, where the inflection-pointlike point appears at  $\phi = M$ .

We now consider the particle mass spectrum of the model at low energies. As we have discussed, the condition of the almost vanishing  $\beta_{\lambda_\Phi}(M)$  leads to the relationship of  $Y_M(M) \approx 32^{1/4} g_X(M)$ . The low energy mass spectrum of the  $Z'$  boson and the right-handed neutrinos are obtained by extrapolating the couplings to low energies. From Eq. (3.11), with the upper bound on  $M < 5.67 M_P$ , we can see  $g_X(M) \ll 1$ , and hence, the RG running effects of the gauge and Yukawa couplings are negligible and  $m_N/m_{Z'} \approx 0.84$  remains almost the same at low energies. On the other hand, the RG evolution of the inflaton quartic coupling significantly changes its value at low energies (as shown in the left panel of Fig. 2), since its beta function is controlled by the gauge and Yukawa couplings. Let us approximately solve the RG equations in Eq. (3.12). Since  $g_X(M), Y_M(M) \ll 1$ , the solutions to their RG equations are approximately given by

$$\begin{aligned} g_X(\mu) &\approx g_X(M) + \beta_g(M) \ln \left[ \frac{\mu}{M} \right], \\ Y_M(\mu) &\approx Y_M(M) + \beta_Y(M) \ln \left[ \frac{\mu}{M} \right], \end{aligned} \quad (3.20)$$

where  $\beta_g(M)$  and  $\beta_Y(M)$  are their beta functions evaluated at  $\mu = M$ . Hence, the beta function of the quartic coupling is approximately described as

$$\begin{aligned} \beta_{\lambda_\Phi}(\mu) &\approx 96g_X^4(\mu) - 3Y^4(\mu) \\ &\approx 4(96g_X(M)^3\beta_g(M) - 3Y_M(M)^3\beta_Y(M)) \ln \left[ \frac{\mu}{M} \right] \\ &\approx M\beta'_{\lambda_\Phi}(M) \ln \left[ \frac{\mu}{M} \right] \approx 16\lambda_\Phi(M) \ln \left[ \frac{\mu}{M} \right], \end{aligned} \quad (3.21)$$

where we have used  $M\beta'_{\lambda_\Phi}(M) \approx 16\lambda_\Phi(M)$  in Eq. (3.9). Then we obtain the approximate solution to the RG equation as

$$\begin{aligned} \lambda_\Phi(v_X) &\approx 8\lambda_\Phi(M) \left( \ln \left[ \frac{v_X}{M} \right] \right)^2 \\ &\approx 3.868 \times 10^{-15} \left( \frac{M}{M_P} \right)^2 \left( \ln \left[ \frac{v_X}{M} \right] \right)^2, \end{aligned} \quad (3.22)$$

where we have used Eq. (3.10) and  $v_X \ll M$ . Using  $m_{Z'} = 2g(v_X)v_X = 2g(M)v_X$ , the mass ratio of the  $U(1)_X$  Higgs/inflaton to the  $Z'$  boson is given by

$$\begin{aligned} \frac{m_\phi}{m_{Z'}} &\approx 2.911 \times 10^{-6} \left( \frac{M}{M_P} \right)^{2/3} \\ &\times (87 + 256x_H + 164x_H^2)^{1/6} \ln \left[ \frac{M}{v_X} \right]. \end{aligned} \quad (3.23)$$

#### IV. LHC RUN 2 CONSTRAINTS

If kinematically allowed, the  $Z'$  boson in the minimal  $U(1)_X$  model can be produced at the LHC. The ATLAS and CMS Collaborations have been searching for a narrow resonance with dilepton final states at the LHC Run 2 and set the upper limits of a  $Z'$  boson production cross section [24,25]. In the analysis by the ATLAS and CMS Collaborations, the so-called sequential SM  $Z'$  ( $Z'_{\text{SSM}}$ ) model [26] has been considered as a reference model, where the  $Z'$  boson has the same couplings with the SM fermions as the SM  $Z$  boson. In this section, we interpret the current LHC constraints on the sequential  $Z'$  boson into the  $U(1)_X$   $Z'$  boson to identify an allowed parameter region. Then, we examine a consistency of the inflection-point inflation scenario with the LHC Run 2 constraints.

We first calculate the cross section for the process  $pp \rightarrow Z' + X \rightarrow \ell^+\ell^- + X$ . The differential cross section with respect to the invariant mass  $M_{\ell\ell}$  of the final state dilepton is given by

$$\begin{aligned} \frac{d\sigma}{dM_{\ell\ell}} &= \sum_{q,\bar{q}} \int_{\frac{M_{\ell\ell}^2}{E_{\text{CM}}^2}}^1 dx \frac{2M_{\ell\ell}}{xE_{\text{CM}}} f_q(x, Q^2) f_{\bar{q}}\left(\frac{M_{\ell\ell}^2}{xE_{\text{CM}}^2}, Q^2\right) \\ &\times \hat{\sigma}(q\bar{q} \rightarrow Z' \rightarrow \ell^+\ell^-), \end{aligned} \quad (4.1)$$

where  $f_q$  is the parton distribution function for a parton (quark) “ $q$ ”, and  $E_{\text{CM}} = 13$  TeV is the center-of-mass energy of the LHC Run 2. In our numerical analysis, we employ CTEQ6L [27] for the parton distribution functions with the factorization scale  $Q = m_{Z'}$ . Here, the cross section for the colliding partons is given by

$$\begin{aligned} \hat{\sigma}(q\bar{q} \rightarrow Z' \rightarrow \ell^+\ell^-) &= \frac{\pi}{1296} \alpha_X^2 \frac{M_{\ell\ell}^2}{(M_{\ell\ell}^2 - m_{Z'}^2)^2 + m_{Z'}^2 \Gamma_{Z'}^2} F_{q\ell}(x_H), \end{aligned} \quad (4.2)$$

where  $\alpha_X = g_X^2/(4\pi)$ , the functions  $F_{u\ell}(x_H)$  and  $F_{d\ell}(x_H)$  are

$$\begin{aligned} F_{u\ell}(x_H) &= (8 + 20x_H + 17x_H^2)(8 + 12x_H + 5x_H^2), \\ F_{d\ell}(x_H) &= (8 - 4x_H + 5x_H^2)(8 + 12x_H + 5x_H^2), \end{aligned} \quad (4.3)$$

for  $q$  being the up-type ( $u$ ) and down-type ( $d$ ) quarks, respectively, and the total decay width of  $Z'$  boson is given by

$$\Gamma_{Z'} = \frac{\alpha_X}{6} m_{Z'} \left[ F(x_H) + 3 \left( 1 - \frac{4m_N^2}{m_{Z'}^2} \right)^{\frac{3}{2}} \theta \left( \frac{m_{Z'}}{m_N} - 2 \right) \right], \quad (4.4)$$

with  $F(x_H) = 13 + 16x_H + 10x_H^2$ . By integrating the differential cross section over a range of  $M_{\ell\ell}$  set by the ATLAS and CMS analyses, respectively, we obtain the cross section to be compared with the upper bounds obtained by the ATLAS and CMS Collaborations.

In interpreting the 2016 results by the ATLAS and CMS Collaborations into the  $U(1)_X$   $Z'$  boson case, we follow the strategy in [28] (see also [29] for the minimal  $B-L$  model). In this paper, the cross section for the process  $pp \rightarrow Z'_{\text{SSM}} + X \rightarrow \ell^+\ell^- + X$  is calculated, and the resultant cross sections are scaled by a  $k$ -factor to match with the theoretical predictions presented in the ATLAS and CMS papers. With the  $k$ -factor determined in this way, the cross section for the process  $pp \rightarrow Z' + X \rightarrow \ell^+\ell^- + X$  is calculated to identify an allowed region for the model parameters of  $\alpha_X$ ,  $x_H$  and  $m_{Z'}$ . See Ref. [28] for the details of the strategy and the  $k$ -factors. Our analysis in this section is exactly the same as that in this reference.

For  $m_{Z'} = 4$  TeV, we show in Fig. 3 the upper bounds on  $\alpha_X x_H^2$  as a function of  $x_H$  from the CMS results on a search for a narrow resonance from the combined dielectron and dimuon channels [25]. The lower and upper dashed lines correspond to  $x_H > 0$  and  $x_H < 0$ , respectively. The upper bounds from the ATLAS results [24] are found to be very similar to, but slightly weaker than, those from the CMS results, and we have only shown the CMS

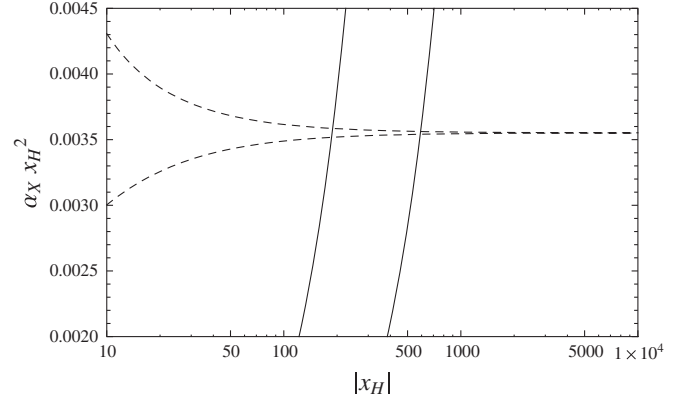


FIG. 3. The upper bounds on  $\alpha_X x_H^2$  as a function of  $x_H$  from the CMS results on a search for a narrow resonance from the combined dielectron and dimuon channels [25]. The lower and upper dashed lines correspond to  $x_H > 0$  and  $x_H < 0$ , respectively. Here we have fixed  $m_{Z'} = 4$  TeV. The diagonal solid lines depict Eq. (3.13) for  $M = M_P$  (left) and  $M = 0.1M_P$  (right), along which the successful inflection-point inflation is achieved.

results. As we can see from the cross section formula, the dashed lines approach each other for a large  $|x_H|$ . The diagonal solid lines depict Eq. (3.10) for  $M = M_P$  (left) and  $M = 0.01M_P$  (right), along which the successful inflection-point inflation is achieved. For the diagonal solid lines with a fixed  $M$ , the results for  $x_H > 0$  and  $x_H < 0$  are indistinguishable. From this figure, we find an upper bound on  $x_H \lesssim 200$  and  $x_H \lesssim 600$ , respectively, for  $M = M_P$  (left) and  $M = 0.01M_P$  (right). Note that even though the successful inflection-point inflation requires the  $U(1)_X$  gauge coupling to be very small, this scenario can still be tested at the LHC when  $|x_H| \gg 1$ , in other words, the  $U(1)_X$  gauge symmetry is oriented towards the SM hyper-charge direction.

## V. CONSTRAINTS FROM THE BIG BANG NUCLEOSYNTHESIS

Let us now consider a reheating scenario after inflation to connect our inflation scenario with the Standard Big Bang cosmology. This occurs via inflaton decay into the SM particles during the inflaton oscillations around its potential minimum. We estimate the reheating temperature ( $T_R$ ) as

$$T_R \approx 0.55 \left( \frac{100}{g_*} \right)^{1/4} \sqrt{\Gamma_\phi M_P}, \quad (5.1)$$

where  $\Gamma_\phi$  is the inflaton decay width into the SM particles. For the successful big bang nucleosynthesis (BBN), we impose a model-independent lower bound on the reheating temperature as  $T_R \gtrsim 1$  MeV.

In the Higgs potential of Eq. (3.3), a mass matrix between the inflaton ( $\phi$ ) and the SM Higgs boson ( $h$ ) is generated after the  $U(1)_X$  symmetry and the electroweak symmetry breaking shown by:

$$\mathcal{L} \supset -\frac{1}{2} \begin{bmatrix} h & \phi \end{bmatrix} \begin{bmatrix} m_h^2 & \lambda_{\text{mix}} v_h v_X \\ \lambda_{\text{mix}} v_h v_X & m_\phi^2 \end{bmatrix} \begin{bmatrix} h \\ \phi \end{bmatrix}, \quad (5.2)$$

where  $m_\phi = \sqrt{2\lambda_\phi} v_X$ , and  $m_h = \sqrt{2\lambda_H} v_h = 125$  GeV. We diagonalize the mass matrix by

$$\begin{bmatrix} h \\ \phi \end{bmatrix} = \begin{bmatrix} \cos \theta & \sin \theta \\ -\sin \theta & \cos \theta \end{bmatrix} \begin{bmatrix} \phi_1 \\ \phi_2 \end{bmatrix}, \quad (5.3)$$

where  $\phi_1$  and  $\phi_2$  are the mass eigenstates. The relationships among the mass parameters and the mixing angle ( $\theta$ ) are the following:

$$\begin{aligned} 2v_h v_X \lambda_{\text{mix}} &= (m_h^2 - m_\phi^2) \tan 2\theta, \\ m_{\phi_1}^2 &= m_h^2 - (m_\phi^2 - m_h^2) \frac{\sin^2 \theta}{1 - 2\sin^2 \theta}, \\ m_{\phi_2}^2 &= m_\phi^2 + (m_\phi^2 - m_h^2) \frac{\sin^2 \theta}{1 - 2\sin^2 \theta}. \end{aligned} \quad (5.4)$$

Since the inflaton is much lighter than the  $Z'$  boson and the heavy neutrinos, it decays to the SM particles mainly through the mixing with the SM Higgs boson. We calculate the inflaton decay width as

$$\Gamma_{\phi_2} = \sin^2 \theta \times \Gamma_h(m_{\phi_2}), \quad (5.5)$$

where  $\Gamma_h(m_{\phi_2})$  is the SM Higgs boson decay width if the SM Higgs boson mass were  $m_{\phi_2}$ .

There are constraints on the mixing angle. Firstly, we have imposed  $\lambda_{\text{mix}}^2 \ll 48g_X^4$  to neglect the contribution of the  $\lambda_{\text{mix}}$  to  $\beta_\phi$ . Another constraint on the mixing angle is from requiring positive definiteness of mass squared eigenvalues of the mass matrix in Eq. (5.2), which leads to  $\lambda_{\text{mix}}^2 < 4\lambda_H\lambda_\phi$ . We find that the latter constraint is more severe and requires  $\theta \ll 1$ . Hence  $\phi_1$  and  $\phi_2$  are mostly the SM Higgs and the  $U(1)_X$  Higgs mass eigenstates, respectively.

In the following analysis we parametrize  $\lambda_{\text{mix}}^2 = 4\lambda_H\lambda_\phi\xi$  with a new parameter  $0 < \xi < 1$ . From Eq. (5.4), we obtain

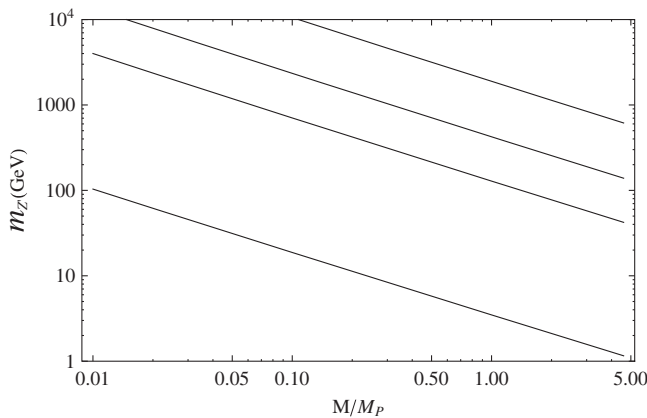


FIG. 4. The contours corresponding to the reheating temperatures  $T_R = 1$  MeV, 1 GeV, 100 GeV, and 1 TeV, from bottom to top, for  $x_H = 400$  and  $\xi = 0.1$ .

$$\theta^2 \approx \xi \left( \frac{m_\phi}{m_h} \right)^2, \quad (5.6)$$

where we have used  $m_\phi^2 \ll m_h^2$  from Eq. (3.23) for the parameter region we are interested in, namely  $m_{Z'} = \mathcal{O}(1 \text{ TeV})$ . We also find that  $m_{\phi_2} \approx m_\phi \sqrt{1 - \xi}$ . From Eqs. (3.23), (5.1), (5.5), and (5.6), we can express the reheating temperature as a function of  $M$ ,  $m_{Z'}$ ,  $x_H$ , and  $\xi$ . To simplify our analysis, let us fix  $x_H = 400$  and  $\xi = 0.1$ . In Fig. 4, we show the contours corresponding to  $T_R = 1$  MeV, 1 GeV, 100 GeV, and 1 TeV, from bottom to top.

## VI. CONCLUSIONS

From a theoretical point of view, if the inflaton value is trans-Planckian, effective operators suppressed by the Planck mass could significantly affect the inflaton potential during inflation, and hence, the inflationary predictions. To avoid this problem, we may consider the SFI, where the inflaton value during inflation is smaller than the Planck mass. In this case, the inflection-point inflation is an interesting possibility to realize a successful slow-roll inflation when inflation is driven by a single scalar field. To realize the inflection-pointlike behavior for the RG improved effective  $\lambda\phi^4$  potential, the running quartic coupling  $\lambda(\phi)$  must exhibit a minimum with an almost vanishing value in its RG evolution, namely  $\lambda(\phi_I) \approx 0$  and  $\beta_\lambda(\phi_I) \approx 0$ , where  $\beta_\lambda$  is the beta function of the quartic coupling.

From a particle physics perspective, it is more compelling to consider an inflationary scenario, where the inflaton field plays another important role. We may consider a general Higgs model, namely the gauge Higgs-Yukawa system, and identify the Higgs field as inflaton. In this case, the conditions,  $\lambda(\phi_I) \approx 0$  and  $\beta_\lambda(\phi_I) \approx 0$ , lead to a relationship among the gauge, the Yukawa, and the Higgs quartic couplings. Using the relationship and requiring the inflationary predictions to be consistent with the Planck 2015 results, we have found that all of the couplings (at  $\phi_I$ ) depend only on  $\phi_I$ . Hence, the low energy mass spectrum of the model is uniquely determined by only two free parameters,  $\phi_I$  and the inflaton/Higgs VEV, and the inflationary predictions are complementary to the low energy mass spectrum. It is also interesting that the inflection-point inflation provides a unique prediction for the running of the spectral index  $\alpha \approx -2.7 \times 10^{-3}$ , which can be tested in future experiments.

We have investigated the inflection-point inflation in the context of the minimal  $U(1)_X$  extended SM, where the anomaly free, extra gauge symmetry is defined as a linear combination of the SM hypercharge and the gauged  $B - L$  groups. Identifying the  $U(1)_X$  Higgs field with the inflaton, we have obtained a prediction for the mass spectrum for the  $Z'$  boson, the right-handed neutrinos, and the  $U(1)_X$  Higgs boson as a function of  $\phi_I$ ,  $x_H$ , and the inflaton/Higgs VEV. Even though the successful inflection-point inflation requires the  $U(1)_X$  gauge coupling to be very small, we

have found that the  $Z'$  boson with mass of a few TeV can be explored at the LHC Run 2 when the direction of the  $U(1)_X$  symmetry is oriented towards the SM hypercharge, or equivalently  $|x_H| \gg 1$ . This is in sharp contrast to the inflection-point inflation scenario in the minimal  $U(1)_{B-L}$  extended SM, previously investigated in Ref. [16]. We have also considered the reheating after inflation and found a large portion of parameter space that can reheat the universe sufficiently high.

### ACKNOWLEDGMENTS

S. O. would like to thank the Department of Physics and Astronomy at the University of Alabama for their

hospitality during her visit for the completion of this work. She would also like to thank the FUSUMA Alumni Association at Yamagata University for travel support for her visit to the University of Alabama. This work is supported in part by the United States Department of Energy (Award No. DE-SC0013680).

### APPENDIX: RG EQUATIONS IN THE MINIMAL $U(1)_X$ MODEL

In this Appendix we list the one-loop RG equations for the couplings which are used in our analysis. See Appendix in Ref. [30] for a complete list. The RG equations for the gauge couplings at the one-loop level are given by

$$\begin{aligned}
\mu \frac{dg_1}{d\mu} &= \frac{g_1}{(4\pi)^2} \left[ 12 \left( \frac{1}{6} g_1 + x_q \tilde{g} \right)^2 + 6 \left( \frac{2}{3} g_1 + x_u \tilde{g} \right)^2 + 6 \left( -\frac{1}{3} g_1 + x_d \tilde{g} \right)^2 \right. \\
&\quad \left. + 4 \left( -\frac{1}{2} g_1 + x_\ell \tilde{g} \right)^2 + 2(x_\nu \tilde{g})^2 + 2(-g_1 + x_e \tilde{g})^2 + \frac{2}{3} \left( \frac{1}{2} g_1 + x_H \tilde{g} \right)^2 + \frac{1}{3} (x_\Phi \tilde{g})^2 \right], \\
\mu \frac{dg_X}{d\mu} &= \frac{g_X^3}{(4\pi)^2} \left[ 12x_q^2 + 6x_u^2 + 6x_d^2 + 4x_\ell^2 + 2x_\nu^2 + 2x_e^2 + \frac{2}{3}x_H^2 + \frac{1}{3}x_\Phi^2 \right], \\
\mu \frac{d\tilde{g}}{d\mu} &= \frac{1}{(4\pi)^2} \left[ \tilde{g} \left\{ 12 \left( \frac{1}{6} g_1 + x_q \tilde{g} \right)^2 + 6 \left( \frac{2}{3} g_1 + x_u \tilde{g} \right)^2 + 6 \left( -\frac{1}{3} g_1 + x_d \tilde{g} \right)^2 \right. \right. \\
&\quad \left. \left. + 4 \left( -\frac{1}{2} g_1 + x_\ell \tilde{g} \right)^2 + 2(x_\nu \tilde{g})^2 + 2(-g_1 + x_e \tilde{g})^2 + \frac{2}{3} \left( \frac{1}{2} g_1 + x_H \tilde{g} \right)^2 + \frac{1}{3} (x_\Phi \tilde{g})^2 \right\} \right. \\
&\quad \left. + 2g_X^2 \left\{ 12x_q \left( \frac{1}{6} g_1 + x_q \tilde{g} \right) + 6x_u \left( \frac{2}{3} g_1 + x_u \tilde{g} \right) + 6x_d \left( -\frac{1}{3} g_1 + x_d \tilde{g} \right) + 4x_\ell \left( -\frac{1}{2} g_1 + x_\ell \tilde{g} \right) \right. \right. \\
&\quad \left. \left. + 2x_\nu(x_\nu \tilde{g}) + 2x_e(-g_1 + x_e \tilde{g}) + \frac{2}{3}x_H \left( \frac{1}{2} g_1 + x_H \tilde{g} \right) + \frac{1}{3}x_\Phi(x_\Phi \tilde{g}) \right\} \right]. \tag{A1}
\end{aligned}$$

Here,  $x_f$  is a  $U(1)_X$  charge of a corresponding fermion ( $f$ ) in Table I. For example,  $x_q = (1/6)x_H + (1/3)x_\Phi$ , and  $x_e = -x_H - x_\Phi$ . For the RG equations for the Majorana Yukawa couplings at the one-loop level we have

$$\mu \frac{dY_M^i}{d\mu} = \frac{Y_M^i}{(4\pi)^2} \left[ (Y_M^i)^2 + \frac{1}{2} \sum_{j=1}^3 (Y_M^j)^2 + (12x_\nu^2 - 6x_\Phi^2)(\tilde{g}^2 + g_X^2) \right]. \tag{A2}$$

Finally, the RG equations for the scalar quartic couplings are given by

$$\begin{aligned}
\mu \frac{d\lambda_\Phi}{d\mu} &= \frac{1}{(4\pi)^2} \left[ \lambda_\Phi \left\{ 20\lambda_\Phi + 2 \sum_{i=1}^3 (Y_M^i)^2 - 12(x_\Phi \tilde{g})^2 - 12(x_\Phi g_X)^2 \right\} + 2\lambda_{\text{mix}}^2 - 4 \sum_{i=1}^3 (Y_M^i)^4 + 6\{(x_\Phi \tilde{g})^2 + (x_\Phi g_X)^2\}^2 \right], \\
\mu \frac{d\lambda_{\text{mix}}}{d\mu} &= \frac{1}{(4\pi)^2} \left[ \lambda_{\text{mix}} \left\{ 12\lambda_H + 8\lambda_\Phi + 4\lambda_{\text{mix}} + 6y_t^2 + \sum_{i=1}^3 (Y_M^i)^2 - \frac{9}{2}g_2^2 - 6 \left( \frac{1}{2}g_1 + x_H \tilde{g} \right)^2 - 6(x_\Phi \tilde{g})^2 - 6(x_H g_X)^2 - 6(x_\Phi g_X)^2 \right\} \right. \\
&\quad \left. + 12 \left\{ \left( \frac{1}{2}g_1 + x_H \tilde{g} \right) (x_\Phi \tilde{g}) + (x_H g_X)(x_\Phi g_X) \right\}^2 \right]. \tag{A3}
\end{aligned}$$

- [1] A. A. Starobinsky, A New Type of Isotropic Cosmological Models Without Singularity, *Phys. Lett.* **91B**, 99 (1980).
- [2] A. H. Guth, The inflationary universe: A possible solution to the horizon and flatness problems, *Phys. Rev. D* **23**, 347 (1981).
- [3] A. D. Linde, Chaotic Inflation, *Phys. Lett.* **129B**, 177 (1983).
- [4] A. Albrecht and P. J. Steinhardt, Cosmology for Grand Unified Theories with Radiatively Induced Symmetry Breaking, *Phys. Rev. Lett.* **48**, 1220 (1982).
- [5] A. D. Linde, Hybrid inflation, *Phys. Rev. D* **49**, 748 (1994).
- [6] R. Allahverdi, K. Enqvist, J. Garcia-Bellido, and A. Mazumdar, Gauge Invariant MSSM Inflation, *Phys. Rev. Lett.* **97**, 191304 (2006); R. Allahverdi, K. Enqvist, J. Garcia-Bellido, A. Jokinen, and A. Mazumdar, MSSM flat direction inflation: Slow roll, stability, fine tuning and reheating, *J. Cosmol. Astropart. Phys.* **06** (2007) 019; J. C. Bueno Sanchez, K. Dimopoulos, and D. H. Lyth, A-term inflation and the MSSM, *J. Cosmol. Astropart. Phys.* **01** (2007) 015; D. Baumann, A. Dymarsky, I. R. Klebanov, L. McAllister, and P. J. Steinhardt, A Delicate Universe, *Phys. Rev. Lett.* **99**, 141601 (2007); D. Baumann, A. Dymarsky, I. R. Klebanov, and L. McAllister, Towards an explicit model of D-brane inflation, *J. Cosmol. Astropart. Phys.* **01** (2008) 024; M. Badziak and M. Olechowski, Volume modulus inflection point inflation and the gravitino mass problem, *J. Cosmol. Astropart. Phys.* **02** (2009) 010; K. Enqvist, A. Mazumdar, and P. Stephens, Inflection point inflation within supersymmetry, *J. Cosmol. Astropart. Phys.* **06** (2010) 020; R. Cerezo and J. G. Rosa, Warm inflection, *J. High Energy Phys.* **01** (2013) 024; S. Choudhury, A. Mazumdar, and S. Pal, Low & high scale MSSM inflation, gravitational waves and constraints from Planck, *J. Cosmol. Astropart. Phys.* **07** (2013) 041; S. Choudhury and A. Mazumdar, Reconstructing inflationary potential from BICEP2 and running of tensor modes, [arXiv:1403.5549](https://arxiv.org/abs/1403.5549).
- [7] G. Ballesteros and C. Tamarit, Radiative plateau inflation, *J. High Energy Phys.* **02** (2016) 153.
- [8] S. M. Choi and H. M. Lee, Inflection point inflation and reheating, *Eur. Phys. J. C* **76**, 303 (2016).
- [9] F. L. Bezrukov and M. Shaposhnikov, The Standard Model Higgs Boson as the Inflation, *Phys. Lett. B* **659**, 703 (2008); J. Garcia-Bellido, D. G. Figueroa, and J. Rubio, Preheating in the standard model with the Higgs-inflaton coupled to gravity, *Phys. Rev. D* **79**, 063531 (2009); F. Bezrukov, D. Gorbunov, and M. Shaposhnikov, On initial conditions for the hot big bang, *J. Cosmol. Astropart. Phys.* **06** (2009) 029; F. L. Bezrukov, A. Magnin, and M. Shaposhnikov, Standard Model Higgs Boson Mass from Inflation, *Phys. Lett. B* **675**, 88 (2009); F. Bezrukov and M. Shaposhnikov, Standard model Higgs boson mass from inflation: Two loop analysis, *J. High Energy Phys.* **07** (2009) 089; F. Bezrukov, A. Magnin, M. Shaposhnikov, and S. Sibiryakov, Higgs inflation: Consistency and generalisations, *J. High Energy Phys.* **01** (2011) 016; F. Bezrukov and M. Shaposhnikov, Higgs Inflation at the Critical Point, *Phys. Lett. B* **734**, 249 (2014); Y. Hamada, H. Kawai, K.-y. Oda, and S. C. Park, Higgs Inflation is Still Alive After the Results from BICEP2, *Phys. Rev. Lett.* **112**, 241301 (2014).
- [10] A. O. Barvinsky, A. Y. Kamenshchik, and A. A. Starobinsky, Inflation scenario via the standard model Higgs boson and LHC, *J. Cosmol. Astropart. Phys.* **11** (2008) 021; A. O. Barvinsky, A. Y. Kamenshchik, C. Kiefer, A. A. Starobinsky, and C. Steinwachs, Asymptotic freedom in inflationary cosmology with a non-minimally coupled Higgs field, *J. Cosmol. Astropart. Phys.* **12** (2009) 003; A. O. Barvinsky, A. Y. Kamenshchik, C. Kiefer, A. A. Starobinsky, and C. F. Steinwachs, Higgs boson, renormalization group, and naturalness in cosmology, *Eur. Phys. J. C* **72**, 2219 (2012).
- [11] A. De Simone, M. P. Hertzberg, and F. Wilczek, Running Inflation in the Standard Model, *Phys. Lett. B* **678**, 1 (2009); T. E. Clark, B. Liu, S. T. Love, and T. ter Veldhuis, The standard model Higgs boson-inflaton and dark matter, *Phys. Rev. D* **80**, 075019 (2009).
- [12] M. Sher, Electroweak Higgs potentials and vacuum stability, *Phys. Rep.* **179**, 273 (1989).
- [13] N. Okada, M. U. Rehman, and Q. Shafi, Tensor to scalar ratio in non-minimal  $\phi^4$  inflation, *Phys. Rev. D* **82**, 043502 (2010); N. Okada, V. N. Senoguz, and Q. Shafi, The observational status of simple inflationary models: An update, *Turk. J. Phys.* **40**, 150 (2016); T. Inagaki, R. Nakanishi, and S. D. Odintsov, Non-Minimal Two-Loop Inflation, *Phys. Lett. B* **745**, 105 (2015).
- [14] K. Kannike, G. Hutsi, L. Pizza, A. Racioppi, M. Raidal, A. Salvio, and A. Strumia, Dynamically induced Planck scale and inflation, *J. High Energy Phys.* **05** (2015) 065; N. Okada and D. Raut, Running non-minimal inflation with stabilized inflaton potential, *Proc. Sci.*, DSU2015 (2016) 013; K. Kannike, A. Racioppi, and M. Raidal, Linear inflation from quartic potential, *J. High Energy Phys.* **01** (2016) 035.
- [15] R. N. Mohapatra and R. E. Marshak, Local B-L Symmetry of Electroweak Interactions, Majorana Neutrinos and Neutron Oscillations, *Phys. Rev. Lett.* **44**, 1316 (1980); Erratum, *Phys. Rev. Lett.* **44**, 1643(E) (1980); R. E. Marshak and R. N. Mohapatra, Quark—Lepton Symmetry and B-L as the U(1) Generator of the Electroweak Symmetry Group, *Phys. Lett.* **91B**, 222 (1980); C. Wetterich, Neutrino Masses and the Scale of B-L Violation, *Nucl. Phys.* **B187**, 343 (1981); A. Masiero, J. F. Nieves, and T. Yanagida,  $B-1$  Violating Proton Decay and Late Cosmological Baryon Production, *Phys. Lett.* **116B**, 11 (1982); R. N. Mohapatra and G. Senjanovic, Spontaneous breaking of global  $B-1$  symmetry and matter—antimatter oscillations in grand unified theories, *Phys. Rev. D* **27**, 254 (1983); W. Buchmuller, C. Greub, and P. Minkowski, Neutrino Masses, Neutral Vector Bosons and the Scale of B-L Breaking, *Phys. Lett. B* **267**, 395 (1991).
- [16] N. Okada and D. Raut, Inflection-point Higgs Inflation, *Phys. Rev. D* **95**, 035035 (2017).
- [17] B. Schmidt, The high-luminosity upgrade of the LHC: Physics and technology challenges for the accelerator and the experiments, *J. Phys. Conf. Ser.* **706**, 022002 (2016).
- [18] M. Anelli *et al.* (SHiP Collaboration), A facility to search for hidden particles (SHiP) at the CERN SPS, [arXiv:1504.04956](https://arxiv.org/abs/1504.04956).
- [19] T. Appelquist, B. A. Dobrescu, and A. R. Hopper, Nonexotic neutral gauge bosons, *Phys. Rev. D* **68**, 035012 (2003).
- [20] P. A. R. Ade *et al.* (Planck Collaboration), Planck 2015 results. XIII. Cosmological parameters, *Astron. Astrophys.* **594**, A13 (2016).

- [21] K. N. Abazajian *et al.*, Inflation physics from the cosmic microwave background and large scale structure, *Astropart. Phys.* **63**, 55 (2015).
- [22] P. Minkowski,  $\mu \rightarrow e\gamma$  at a rate of one out of  $10^9$  muon decays?, *Phys. Lett.* **67B**, 421 (1977); T. Yanagida, in *Proceedings of the Workshop on the Unified Theory and the Baryon Number in the Universe*, edited by O. Sawada and A. Sugamoto (KEK, Tsukuba, Japan, 1979), p. 95; M. Gell-Mann, P. Ramond, and R. Slansky, *Supergravity*, edited by P. van Nieuwenhuizen *et al.* (North-Holland, Amsterdam, 1979), p. 315; S. L. Glashow, The Future of Elementary Particle Physics, in *Proceedings of the 1979 Cargèse Summer Institute on Quarks and Leptons*, edited by M. Lévy *et al.*, (Plenum Press, New York, 1980), p. 687; R. N. Mohapatra and G. Senjanović, Neutrino Mass and Spontaneous Parity Violation, *Phys. Rev. Lett.* **44**, 912 (1980); J. Schechter and J. W. F. Valle, Neutrino masses in  $SU(2) \times U(1)$  theories, *Phys. Rev. D* **22**, 2227 (1980).
- [23] SLD Electroweak Group, SLD Heavy Flavor Group, DELPHI, LEP, ALEPH, OPAL, LEP Electroweak Working Group, and L3 Collaboration, A Combination of preliminary electroweak measurements and constraints on the standard model, [arXiv:hep-ex/0312023](https://arxiv.org/abs/hep-ex/0312023); S. Schael *et al.* (ALEPH and DELPHI and L3 and OPAL and LEP Electroweak Collaborations), Electroweak measurements in electron-positron collisions at W-Boson-Pair Energies at LEP, *Phys. Rep.* **532**, 119 (2013).
- [24] ATLAS Collaboration [ATLAS Collaboration], Search for new high-mass resonances in the dilepton final state using proton-proton collisions at  $\sqrt{s} = 13$  TeV with the ATLAS detector, Report No. ATLAS-CONF-2016-045.
- [25] CMS Collaboration [CMS Collaboration], Search for a high-mass resonance decaying into a dilepton final state in  $13 \text{ fb}^{-1}$  of pp collisions at  $\sqrt{s} = 13$  TeV, Report No. CMS-PAS-EXO-16-031.
- [26] V. D. Barger, W. Y. Keung, and E. Ma, Doubling of Weak Gauge Bosons in an Extension of the Standard Model, *Phys. Rev. Lett.* **44**, 1169 (1980).
- [27] J. Pumplin, D. R. Stump, J. Huston, H. L. Lai, P. M. Nadolsky, and W. K. Tung, New generation of parton distributions with uncertainties from global QCD analysis, *J. High Energy Phys.* **07** (2002) 012.
- [28] N. Okada and S. Okada,  $Z'$ -portal right-handed neutrino dark matter in the minimal  $U(1)_X$  extended Standard Model, *Phys. Rev. D* **95**, 035025 (2017).
- [29] N. Okada and S. Okada,  $Z'_{BL}$  portal dark matter and LHC Run-2 results, *Phys. Rev. D* **93**, 075003 (2016).
- [30] S. Oda, N. Okada, and D.-s. Takahashi, Classically conformal  $U(1)$  extended standard model and Higgs vacuum stability, *Phys. Rev. D* **92**, 015026 (2015).